The role of North Atlantic-European weather regimes in the surface impact of sudden stratospheric warming events

Daniela I.V. Domeisen[1,*], Christian M. Grams[2,*], and Lukas Papritz[1,*]

[1]Institute for Atmospheric and Climate Science, ETH Zürich, Switzerland
[2]Institute of Meteorology and Climate Research (IMK-TRO), Department Troposphere Research, Karlsruhe Institute of Technology (KIT), Karlsruhe, Germany
[*]Equally contributing authors

Correspondence: Daniela I.V. Domeisen (daniela.domeisen@env.ethz.ch)

Abstract. Sudden stratospheric warming (SSW) events can significantly impact tropospheric weather for a period of several weeks, in particular in the North Atlantic European (NAE) region. While the stratospheric forcing often projects onto the North Atlantic Oscillation (NAO), the tropospheric response to SSW events, if any, is highly variable and it remains an open question what determines the existence, location, timing, and strength of the downward impact. We here explore how the variable tropospheric response to SSW events in the NAE region can be characterised in terms of a refined set of seven weather regimes and if the tropospheric flow in the North Atlantic region at the onset of SSW events is an indicator of the subsequent downward impact. The weather regime analysis reveals the Greenland blocking (GL) and Atlantic Trough (AT) regimes as the most frequent large-scale patterns in the weeks following an SSW. While the GL regime is dominated by high pressure over Greenland, AT is dominated by a southeastward shifted storm track in the North Atlantic. The flow evolution associated with GL and the associated cold conditions over Europe in the weeks following an SSW occur most frequently if a blocking situation over western Europe and the North Sea (European Blocking) prevailed at the time of the SSW onset. In contrast, an AT regime associated with mild conditions is more likely if GL occurs already at SSW onset. For the remaining tropospheric flow regimes during SSW onset we cannot identify a dominant flow evolution. Although it remains unclear what causes these relationships, the results suggest that specific tropospheric states during the onset of the SSW are an indicator of the subsequent tropospheric flow evolution in the aftermath of an SSW, which could provide crucial guidance for subseasonal prediction.

1 Introduction

Sudden stratospheric warming events can have a significant impact on the tropospheric large-scale circulation and hence on surface weather (Baldwin and Dunkerton, 2001). However, a robust detection and quantification of the downward impact of SSWs remains challenging. First of all, the number of SSWs in the record of satellite-era reanalysis is small (26 events from 1979 - 2019), while the case-to-case variability in terms of their tropospheric impact is large. Second, the internal variability

of the troposphere itself is high, such that it can mask a stratospheric influence. Predicting if, when, and where a downward impact from SSW events will occur is therefore not straightforward, yet a better prediction of the type and timing of a downward impact would significantly benefit a wide range of users.

The tropospheric impact of SSW events is communicated by a range of mechanisms including synoptic and planetary-scale waves (e.g. Song and Robinson, 2004; Domeisen et al., 2013; Hitchcock and Simpson, 2014; Smith and Scott, 2016). In particular, after SSW events the North Atlantic-European region (NAE) tends to exhibit more persistent states of the negative phase of the North Atlantic Oscillation (NAO-, Domeisen, 2019), as well as more frequent transitions towards NAO- and fewer away from NAO- (Charlton-Perez et al., 2018). NAO- is associated with enhanced meridional air mass exchanges, in particular, more cold air outbreaks in Northern Europe but fewer over the Nordic Seas (Kolstad et al., 2010; Kretschmer et al., 2018b; Papritz and Grams, 2018; Huang and Tian, 2019), as well as increased precipitation in Southern Europe (Butler et al., 2017; Ayarzagüena et al., 2018). The Pacific sector tends to be less strongly affected in the aftermath of SSW events (Greatbatch et al., 2012; Butler et al., 2017), though the occurrence of wave reflection in the stratosphere can be associated with Pacific blocking (Kodera et al., 2016) and cold spells over North America (Kretschmer et al., 2018a). Given the preferred occurrence and the increased persistence of certain surface signatures after SSW events as compared to climatology, medium- to long-range predictability over Europe has been suggested to increase after SSW events (Sigmond et al., 2013; Domeisen et al., 2015; Karpechko, 2015; Butler et al., 2016; Scaife et al., 2016; Jia et al., 2017; Beerli et al., 2017; Butler et al., 2019; Domeisen et al., 2020a), although SSW events themselves are often not predictable beyond deterministic lead times (Taguchi, 2014, 2016; Domeisen et al., 2020b).

Despite the preferred occurrence of the negative phase of the NAO, the downward influence of an SSW event on the evolution of the tropospheric flow can be highly variable between events. This issue is further complicated by the fact that there exists a range of different metrics for characterizing the downward impact, with each definition yielding a different set and number of SSW events with apparent surface impacts. In particular, the occurrence and type of downward impact has been investigated with respect to the SSW geometry (Charlton and Polvani, 2007; Mitchell et al., 2013; Maycock and Hitchcock, 2015; Seviour et al., 2016), though no statistically robust differences with respect to wave geometry emerge in the tropospheric response. More promising pathways include SSW precursors (Nakagawa and Yamazaki, 2006; White et al., 2019), the evolution of the stratosphere - troposphere system following the SSW (Kodera et al., 2016), and in particular the persistence of the lower stratospheric response (Hitchcock et al., 2013a; Karpechko et al., 2017; Runde et al., 2016; Polichtchouk et al., 2018) after the SSW event. These studies use indices for the downward effect that are based on exclusively stratospheric or a combination of stratospheric and tropospheric indicators. In this study we will investigate purely tropospheric indicators of downward impact for SSW events. Definitions of a downward impact using tropospheric indicators are generally based on large-scale circulation indices such as the NAO (Charlton-Perez et al., 2018; Domeisen, 2019) or tropospheric jet location (Garfinkel et al., 2013; Afargan-Gerstman and Domeisen, 2020; Maycock et al., 2020).

While a causal downward link from the stratosphere after SSW events has been confirmed in idealized experiments (e.g. Gerber et al., 2009), remote forcings can affect both the stratosphere and the troposphere, and thereby either mask or strengthen the downward response from the stratosphere. Indeed, a range of tropical remote connections can impact the NAE region

through both a tropospheric and a stratospheric pathway (Attard et al., 2019), such as the Quasi-Biennial Oscillation (QBO) (Gray et al., 2018; Andrews et al., 2019), the MJO (Garfinkel et al., 2014; Barnes et al., 2019), and the El Niño Southern Oscillation (ENSO) (Jiménez-Esteve and Domeisen, 2018; Domeisen et al., 2019), in addition to extratropical tropospheric forcing in the North Pacific (Honda and Nakamura, 2001; Sun and Tan, 2013; Drouard et al., 2013), Arctic sea ice (Sun et al., 2015), and snow cover in Eurasia (Cohen et al., 2014). It therefore has to be kept in mind that the stratosphere is often only one possible forcing of the troposphere. In addition, it has recently been suggested that the precursors to SSW events with a downward influence differ from those without such a tropospheric impact in terms of strength and location (Domeisen, 2019; Zhang et al., 2019), in particular with respect to forcing over Eurasia (White et al., 2019; Tyrrell et al., 2019; Peings, 2019).

Given the large variability of the tropospheric flow evolution following SSW events and the influence of other remote factors mentioned above, the prediction of the SSW response in the troposphere is difficult for an individual event, despite the general shift towards NAO negative conditions in a statistical sense. The goal of this study is to investigate if tropospheric flow regimes in the NAE region help to understand the variability of the SSW response in the observational record. More specifically, we here address the question if the tropospheric flow evolution in the NAE region after an SSW is statistically different from that without an SSW using seven weather regimes in the NAE region. Weather regimes are quasi-stationary, recurrent, and persistent patterns of the large-scale extratropical circulation (e.g. Michelangeli et al., 1995). While many studies showed that there are preferred transitions between different regimes, internal tropospheric variability is high and a regime onset often occurs on short timescales (e.g. Vautard, 1990; Michel and Rivière, 2011). Therefore predictability due to regimes arises from regime persistence on time scales of several days rather than typical regime sequences over several weeks. However, recent work revealed important shifts of regime occurrence and transition probabilities between regimes on subseasonal time scales of several weeks dependent on the external forcing such as the stratospheric polar vortex state (Charlton-Perez et al., 2018; Papritz and Grams, 2018; Beerli and Grams, 2019). This motivates the study at hand aiming at investigating if the variability in the tropospheric flow evolution following SSW events can be characterised in terms of the weather regime at the time of SSW onset.

2 Data and Methods

2.1 Data and Classifications

ERA-interim reanalysis (Dee et al., 2011) from 1979 to present is used for all figures. The SSW central dates are identified as the day of reversal of the zonal mean zonal winds to easterly at 10 hPa and 60°N in midwinter (Nov - Mar) for ERA-Interim (1979 - 2019), yielding 26 SSW events for the period 1979-2019. For the period 1979 to 2013, these reversal dates are given in Table 2 in Butler et al. (2017). The SSW central dates for the remaining years are 12-Feb-2018 and 02-Jan-2019.

The tropospheric flow over the NAE region is described in terms of quasi-stationary large-scale flow patterns, given by seven year-round weather regimes defined in Grams et al. (2017) based on six-hourly data for the period 1979-2015. We use this weather regime classification to stratify SSWs according to the large-scale tropospheric flow conditions at their onset. To do so, we select for each SSW the dominant weather regime that is active during at least one 6-hourly time step throughout

the onset day of the SSW (see Table 1). As for the canonical seasonal definition using four regimes (e.g. Michelangeli et al., 1995; Michel and Rivière, 2011; Ferranti et al., 2015; Charlton-Perez et al., 2018), the mean patterns of the seven regimes are based on a k-means clustering in the phase space spanned by the leading seven empirical orthogonal functions (EOFs; explaining 76% of the variance) of 10-day low-pass filtered 500hPa geopotential height anomalies. In addition, the normalized projection (weather regime index I_{WR}) following Michel and Rivière (2011) for each of the seven regimes is employed for defining objective weather regime life cycles and for a filtering of time steps without a clear regime structure ("no regime" category). In essence, an active life cycle requires an I_{WR} above a certain threshold for at least 5 consecutive days (minimum duration for an active regime life cycle) and a continuous increase/decrease during the onset/decay phases (see methods of Grams et al., 2017, for details). As different life cycles can be active simultaneously, in particular during the onset and decay phases, individual days are attributed to a specific regime life cycle only if I_{WR} is also the maximum of all I_{WR}. The life cycle definition allows for a continuous extension of the weather regime attribution to more recent data without repeating the EOF analysis and clustering (here done for the years 2016-2019).

Three of the seven regimes are dominated by a cyclonic 500 hPa geopotential height anomaly ("cyclonic regimes"; cf. Figs. A1a-c): the Atlantic Trough (AT) regime with cyclonic activity shifted towards western Europe, the Zonal regime (ZO), and the Scandinavian Trough (ScTr) regime. The remaining four regimes are dominated by a positive geopotential height anomaly and are referred to as "blocked regimes" (Figs. A1d-g): Atlantic Ridge (AR), European Blocking (EuBL), Scandinavian Blocking (ScBL), and Greenland Blocking (GL).

A potential modulation of the frequency of occurrence of the seven regimes can be understood in terms of the link between the respective regimes and the NAO (Beerli and Grams, 2019, their Figs. 2,6) and the link between the stratospheric polar vortex and the NAO (Charlton-Perez et al., 2018). Since ZO and ScTr project onto NAO+, they are suppressed after a weakening of the stratospheric polar vortex, and vice versa after a strengthening. In contrast, GL strongly projects onto NAO- and is enhanced following a weak stratospheric polar vortex, while it is suppressed in the aftermath of a strong vortex. EuBL and AT do not project strongly onto either NAO phase and are, thus, only weakly modulated by the strength of the stratospheric polar vortex.

2.2 Statistical testing

The rare occurrence of SSWs (26 events during 1979-2019) and the subsequent stratification according to tropospheric flow conditions requires careful statistical testing to extract significant and robust results that are distinct from sampling uncertainty. The overarching questions we address in this study are whether after SSWs the tropospheric flow evolution is different from situations without an SSW and to what extent this depends on the tropospheric state at the time of the SSW. To investigate the latter, we will consider subsamples of all SSWs. Hence, in all cases the relevant null hypothesis is that the flow evolution after SSWs is indistinguishable from that occurring in the absence of an SSW. The testing procedure, thus, comprises the following two steps:

1. First, we assess the *robustness* of the samples by performing a Monte Carlo resampling. For that purpose, we resample the original samples 100 times with repetitions. The number of random samples is chosen according to the maximum

Table 1. Weather Regime at the onset of SSW events in the observational record (1979-2019)

dominant weather regime (lag 0)		SSW central date
Atlantic Trough	(AT)	14.03.1988, 24.01.2009, 24.03.2010
Zonal Regime	(ZO)	21.02.1989, 15.12.1998, 22.02.2008, 12.02.2018
Scandinavian Trough	(ScTr)	26.02.1999, 20.03.2000
Atlantic Ridge	(AR)	04.12.1981, 23.01.1987, 02.01.2019
European Blocking	(EuBL)	22.02.1979, 24.02.1984, 01.01.1985, 11.02.2001, 21.01.2006, 07.01.2013
Scandinavian Blocking	(ScBL)	-
Greenland Blocking	(GL)	04.03.1981, 08.12.1987, 30.12.2001, 24.02.2007, 09.02.2010
no regime at onset	(no)	29.02.1980, 18.01.2003, 05.01.2004

number of possible combinations with repetitions of the smallest subset of SSW events that will be considered in this study ($N = 5$ events corresponding to 126 independent combinations). This yields confidence intervals, estimating the uncertainty inherent in each sample. Due to the small sample size, these confidence intervals are relatively large.

2. Second, we compute 1000 random samples of the same size as the original sample but for random periods with the same weather regime at the central date but no SSW occurring within ± 60 days, yielding estimates of the distributions in the absence of SSWs. Prescribing the same weather regime at the central date for the random samples filters out signals which might result from regime persistence or preferred regime transitions independent of external forcings. Testing for *significance* is done by comparing the confidence intervals and distributions obtained from the random samples for overlap.

Applying this method to geopotential height anomalies, we consider anomalies as robust if the width of the confidence interval is smaller than the amplitude of the anomaly. In addition, the sample mean is significant at, e.g., the 10% level, if the confidence intervals overlap by less than 10% with the Monte Carlo distribution. A similar procedure is applied to test significance of lagged weather regime occurrence.

3 Weather regimes during SSW events

As a first step, we evaluate the sequence of weather regimes from 60 days before to 60 days after an SSW for all 26 SSW cases during 1979-2019 (Fig. 1, cf. Tab. 1). This figure suggests a preferred occurrence of AT (purple) and GL (blue) during the weeks after an SSW compared to the weeks before. This is further emphasized by the 5-day running mean of the anomalous frequency of weather regimes around SSW events, which provides a more complete overview over the modulation of regime frequencies after SSWs (Figure 2). We show the 5-day running mean frequency anomaly to account for the 5-day minimum duration of an active regime life cycle. Different from the testing procedure outlined in Section 2.2, we here consider the distribution of lagged 5-day mean frequencies by selecting for each day in the original sample a random day ± 15 days around the original day of year but from a different winter. In addition, the random day must exhibit the same weather regime as the

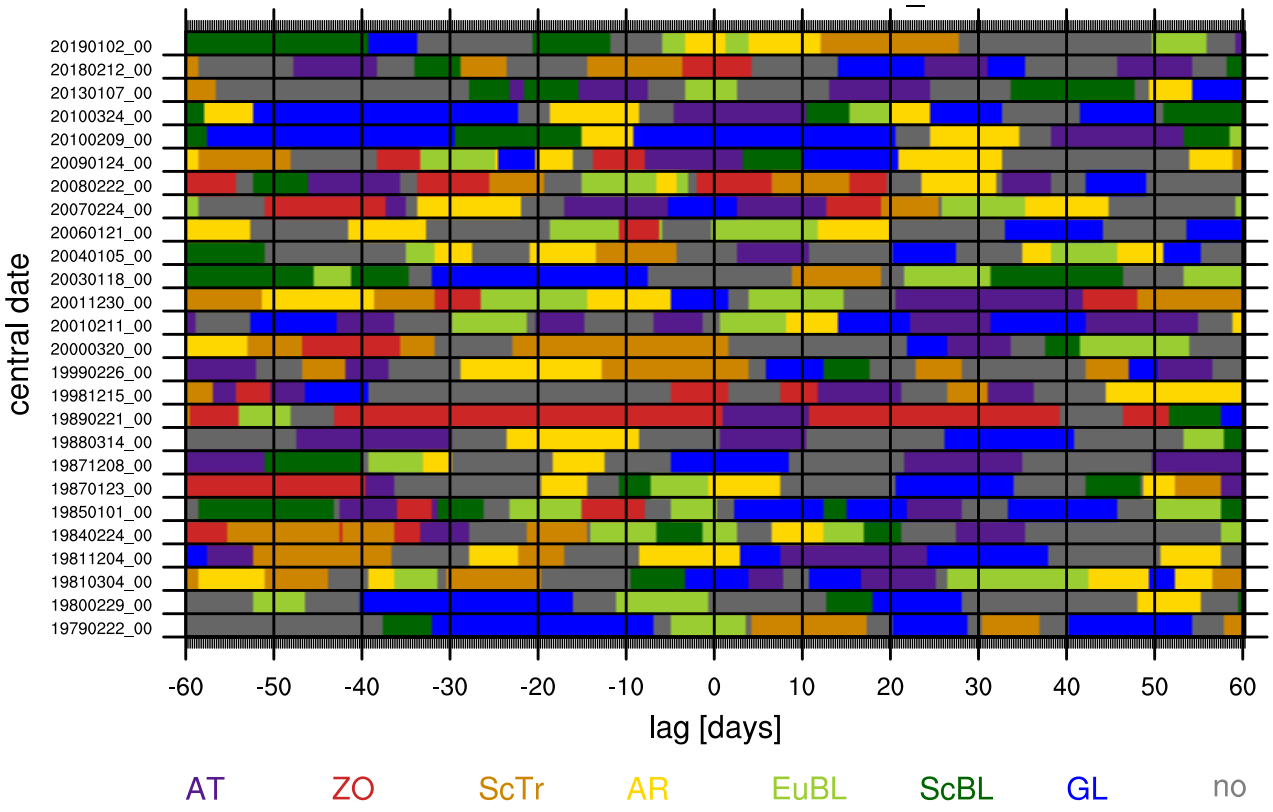

Figure 1. The sequence of the dominant weather regimes (colors indicated in legend) for -60 to +60 days with respect to the onset of each of the 26 SSW events (lag 0) between 1979 and 2019. The central dates of the SSW events are indicated on the left.

original day to replicate potential regime-dependence. We then compute the mean lagged weather regime frequency for each random sample as for the original sample and test for significance at the 10% level (bold). For reference, we show the absolute frequencies of weather regimes in Fig. A2.

GL and EuBL are the most prominent regimes at the onset of SSW events with a relative 5-day mean frequency of more than 18% and 20%, respectively (Figure A2a). The frequency of EuBL is significantly enhanced from 5 days prior until the onset of the SSW (Figure 2a), in agreement with Woollings et al. (2010) and Nishii et al. (2011). The cyclonic regimes ZO, ScTr, as well as the blocked regimes AR and ScBL tend to be suppressed at the time of SSW events. This is consistent with the strong projection of the ZO and ScTr regimes onto NAO+, which also tends to be suppressed after SSW events (Charlton-Perez et al., 2018). On the other hand, AR (yellow, significant peak around lag -20 to -10) and the related ScTr (orange, significant range at lag -10) regimes are more frequent in the period 1-3 weeks before the SSW onset. The prominence of AR around 15 days before the onset of an SSW event agrees with the suggested precursor role of blocking over the Atlantic before SSW events (Martius et al., 2009). After the SSW onset, AT frequencies are significantly enhanced, peaking at more than 23% after 7 days (Figure A2a) corresponding to a frequency anomaly of 15% for the same lag (Figure 2a). Thereafter, GL (lag 12 to 42 days)

and AT (lag 17-35 days) are the most likely weather regimes with enhanced frequency anomalies of up to 15% (Fig. A2a), but in absolute terms frequencies for both are only around 20-25% and none of the two clearly dominates (Figure 2a). This behaviour obscures the potential tropospheric impact of an SSW in a composite as AT and GL trigger contrasting large-scale weather conditions (rather mild and windy for AT, cold and calm for GL) for large parts of Europe (Beerli and Grams, 2019).

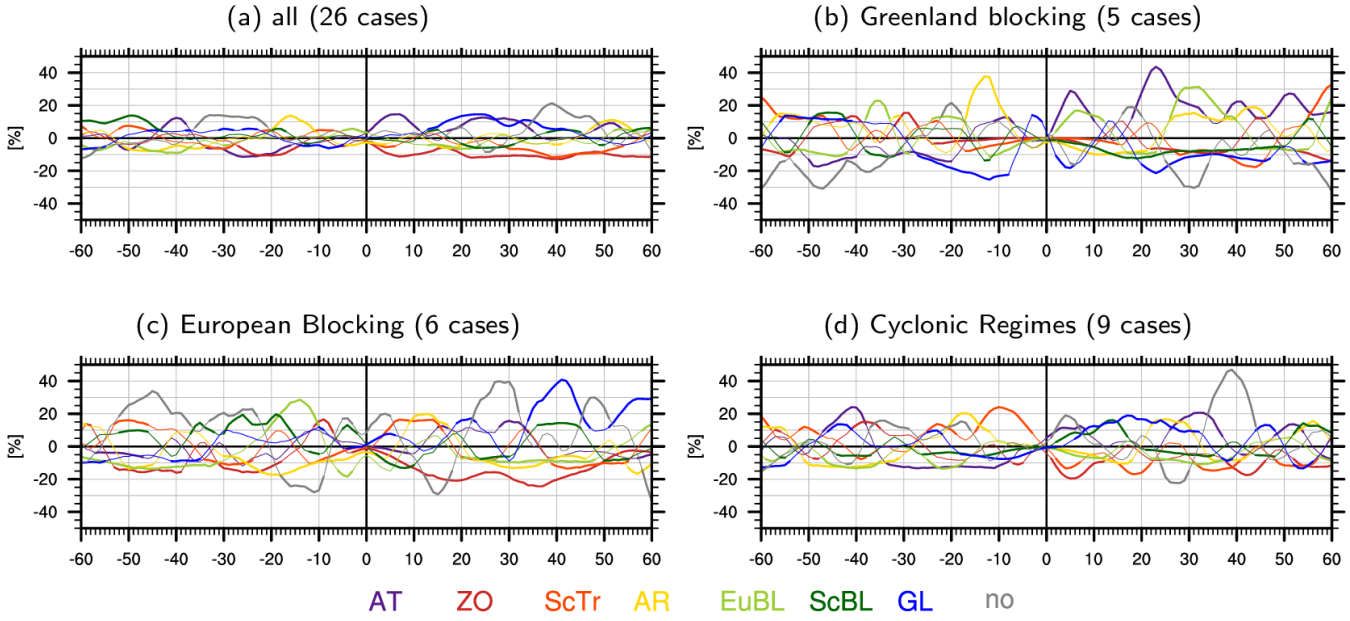

Figure 2. 5-day running mean of the *anomalous* frequency of weather regimes centred on the onset of the SSW event (lag 0) relative to the mean of the climatological distribution for (a) all SSW events and (b-d) conditional on the dominant weather regime at lag 0: (b) Greenland blocking, (c) European blocking, and (d) cyclonic regimes (ZO, AT, and ScTr). The 5-day mean frequencies are computed from 6-hourly weather regime data from lag -60 days to lag 60 days. Note the different y-axis in (a). Note that anomalous frequencies at lag 0 in c, d are - by construction - close to zero as the same regime is prescribed for computing the mean from the 1000 Monte-Carlo samples. The bold parts of the lines indicate significant deviations from climatology (see text for details).

We now sub-divide the 26 SSW events with respect to the weather regime that dominates during the SSW onset: GL (5 cases), EuBL (6 cases), and the cyclonic regimes (ZO, ScTr, AT; 9 cases). The remaining 6 cases either have no clear regime signature (no-regime, 3 events) or are associated with AR (3 events) at their onset. Because of the small sample size, we do not consider these cases here. For the GL subset (Fig. 2b / A2b), all other regimes are subsequently suppressed except for AT and EuBL. The frequency of GL itself drops immediately after the SSW to below 10% around a lag of 20 days – far below its climatological mean frequency. AT, and to a lesser degree also EuBL, become significantly more frequent immediately after the SSW until about a lag of 10 days, reaching absolute frequencies of 35% and 20%, respectively (Fig. A2b). After a period with no clear regime assignment, AT becomes the dominant regime starting at lag 18 days with anomalous frequencies above 40% (Fig. 2b), peaking above 50% absolute frequency about 23 days after the SSW and remaining significantly enhanced until

a lag of 33 days (Fig. A2b). From lag 25 days until lag 40 days, EuBL becomes significantly enhanced peaking at 40% absolute frequency around lag 30 days.

For the EuBL subset (Fig. 2c / A2c), the subsequent regime frequencies are quite different to GL at the onset of an SSW. First, the frequencies of ScTr and AR are significantly enhanced directly after the SSW, with peaks at 20% and 30% absolute frequency at lag 10 days. This is then followed by a period of preferred occurrence of GL (around lag 20 days) and AT (around lag 30 days) with a frequency of about 25% each. The dominance of GL from lag 35 to 45 days (50% peak frequency) is particularly striking. At the same time, also ScBL is enhanced with a frequency of 20%, while all other regimes are suppressed.

Cyclonic regimes at the time of the SSW (Fig. 2d / A2d) exhibit a less prominent regime frequency modulation after an SSW compared to the EuBL and GL subsets. Still, GL (lag 10-35 days, lag 45 days), AR (lag 20-30 days), and AT (lag 25-35 days) are significantly enhanced, but absolute frequencies barely exceed 20%. Note that this corresponds to significantly increased frequencies of 10-20% for these regimes in the considered time windows. However, most often no single regime dominates after an SSW event with a cyclonic regime at lag 0, hinting at cases with a "missing" response after the SSW event.

Despite the large tropospheric variability in the aftermath of SSW events, the investigation of lagged regime frequencies reveals that (1) the AT and GL regimes are more likely to follow an SSW (as compared to other weather regimes) and (2) that this subsequent modulation is sensitive to the tropospheric flow regime at the onset of the SSW. The dominance of EuBL and GL at the time of the SSW onset hints at a significantly more likely GL response (after EuBL at lag 0) vs. AT (after GL at lag 0) after an SSW, respectively. Thus the stratospheric impact on the evolution of the tropospheric flow in the NAE region and hence the associated surface weather may be connected to the presence of a particular tropospheric regime at the onset of the SSW.

4 Temporal Evolution of the Downward Impact

We focus in the following on the modulation of the stratosphere-troposphere coupling for the previously discussed sets of SSWs. For that purpose, we evaluate the temporal evolution of standardized geopotential height anomalies averaged over the NAE sector (-80°E to 40°E / 60°N to 90°N) by compositing a given set of SSW events. Using the full hemisphere, that is, the full longitude range instead of the here used sectorial view over the North Atlantic, yields the same qualitative results due to the strong imprint of the anomalies induced by the SSW in the NAE sector (Fig. A3).

Compositing all SSW events (Fig. 3a) yields the classical dripping paint plot of Baldwin and Dunkerton (2001, their Fig. 2). Qualitative differences to the figure from Baldwin and Dunkerton (2001) are due to the different variable (geopotential height in our study vs NAM) and the number of events (26 in our study vs 18) for a different time period (1979-2019 in our study vs 1958-1999). When compositing all SSW events, the downward impact between 10 to 60 days after the SSW onset is robust at the 25 % but not the 10 % level (see Fig. A4a). Together with the relatively weak amplitude of the anomalies, this reflects the large case-to-case variability in the tropospheric impact of SSWs. A more robust anomaly (10 % level) can only be observed at around 15 days after an SSW. This anomaly around a lag of 15 days is unlikely to be obtained from a random sampling as evident from the less than 10 % overlap between the confidence and random distributions (Fig. 3a). This suggests that in the

immediate aftermath of an SSW (lag 15 - 25 days), indeed positive geopotential height anomalies over the NAE sector are significantly more likely than in the absence of an SSW.

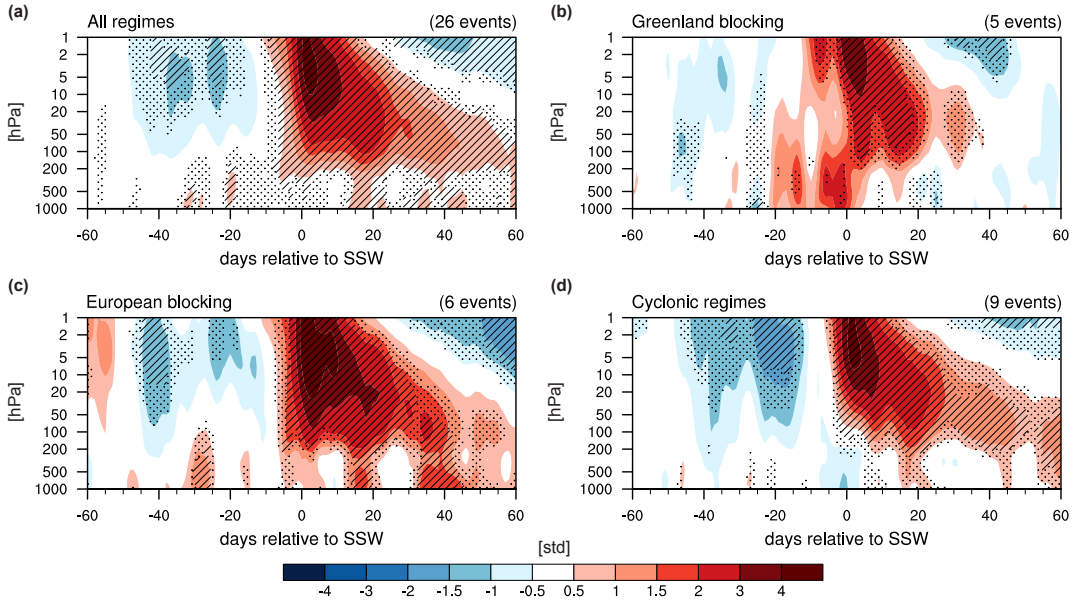

Figure 3. Standardized geopotential height anomalies for the sector -80°E to 40°E / 60°N to 90°N for (a) all SSW events, and (b - d) subdivided by the weather regime that is dominant at the onset of the SSW event as indicated in the panel titles. Hatching (stippling) indicates that the confidence intervals and the random distributions overlap by less than 25% (10%).

SSW events that occur during GL (Fig. 3b) are associated with an immediate, strongly positive anomaly in the troposphere. Consistent with Fig. A2b, when GL is present at the onset of the SSW, GL or AR are often already present before the SSW event, which is likely the cause of the positive tropospheric geopotential height anomalies several days prior to the event. Notably, there are no significant and robust (cf. Figs. 3b and A4b) anomalies after 10 days of the onset of the SSW except for a weak negative geopotential height anomaly after 20 days, indicating a cyclonic flow regime in the NAE region. This is consistent with the significantly enhanced likelihood for the occurrence of the AT regime at this lag (Fig. A2b). Note that both the immediate positive geopotential height anomalies and the weak tropospheric anomalies in the aftermath of the event are not the result of cancellations in the composites but are rather typical across cases.

For EuBL at the onset of the SSW event, only a weakly significant positive anomaly can be observed at the time of the SSW, but highly robust, significant, and strongly positive geopotential height anomalies are present in the troposphere at lags of 15 - 20 and 30 - 55 days after the SSW event (Fig. 3c). These positive anomalies are consistent with the finding that first AR and then GL are much more likely in the aftermath of an SSW with EuBL at lag 0 (compare to Fig. A2c). Furthermore, comparing to the panel for all SSW events (Fig. 3a) indicates that the EuBL cases dominate the perceived downward response in the canonical response for SSW events.

During cyclonic regimes at the onset of the SSW, there is no substantial tropospheric anomaly in the NAE region at the time of the SSW, but a positive albeit weak anomaly can be observed around days 15 - 20 after the SSW event (Fig. 3d). This anomaly is not robust at the 10 % level, but it is significantly different from a random sample at least at the 25 % level. Several SSWs with a cyclonic regime at the onset are followed by GL at a longer lag (Fig. A2d), thus, likely causing these anomalies. Still, the GL frequencies only reach 25% at most and also other regimes occur more often albeit with low frequencies around 25%. These findings and the small amplitude of the anomalies suggest that the variability in the tropospheric flow evolution after SSWs is large after a cyclonic regime at lag 0, which is also confirmed by the inspection of individual cases (not shown).

While not the focus of this study, the question arises whether other factors might contribute to the differing surface evolution in the aftermath of the SSW event. In fact, it is certainly the case that tropospheric variability at SSW onset alone is not responsible for the response to SSWs. In particular, differing values of the amplitude and persistence of the lower stratospheric anomaly can be observed in Fig. 3 between the different composites. In general, the events with EuBL at the onset also tend to have a longer stratospheric persistence, although a long (but slightly weaker) persistence can also be observed for cyclonic regimes at the onset of the SSW. The five SSW events associated with GL have a more short-lived lower stratospheric response. As events with a persistent lower stratospheric response are often associated with so-called polar jet oscillation (PJO) events, a comparison with Table 1 in Karpechko et al. (2017) reveals that 2 out of 5 SSW events with a GL regime (and, respectively, 4 out of 6 EuBl events) at the onset have a persistent lower stratospheric temperature response characterized by a polar jet oscillation (PJO) event (Kuroda and Kodera, 2004; Hitchcock et al., 2013b). While this is not a clear result, it indicates that the shorter (longer) persistence in the lower stratosphere for the SSWs associated with GL (EuBL) may add some support to the persistence of the tropospheric response, but the statistics are too small to provide a clear result. Similarly, 4 out of 6 EuBL events are split events (rather than displacements), while 2 out of 5 GL events are split events.

5 Impact on Surface Weather

Since each weather regime is associated with characteristic surface weather, the modulation of regime successions in the aftermath of an SSW by the tropospheric state at the time of an SSW might contribute to the marked variability in the surface impact. Hence, we here consider spatial composites of 2m temperature anomalies and anomalies of 500 hPa geopotential height (Z500') for the three groups of SSW events discussed in the previous sections (Fig. 4a-c) and for all SSW events (Fig. 4d) for days 0 to 25 after the SSW (cf. Fig. A5 for days 25 - 50).

During SSWs dominated by GL at the onset, initially strong warm anomalies prevail over Greenland and the Canadian Archipelago, whereas western Russia and Scandinavia are anomalously cold, consistent with the anomalous ridge over Greenland and the low geopotential height anomalies over Scandinavia (Fig. 4a). With the subsequent progression of weather regimes - typically towards the cyclonic AT regime or EuBL - mild conditions are established throughout central Europe from a lag of 20 days onwards. This is in stark contrast to the negative NAO and the associated cold conditions that are commonly expected as the canonical response to SSWs over Europe (Butler et al., 2017; Kolstad et al., 2010; Domeisen et al., 2020a).

For SSWs that are dominated by EuBL at the onset, cold anomalies prevail over Northern Europe, albeit also extending over large parts of central Europe (Fig. 4b). They peak at -4 K to -6 K around lags beyond 20 days, which corresponds well with the occurrence of the GL regime. Note that cold anomalies in the composite for all SSWs are much weaker (cf. Fig. 4d) reaching -1 K to -3 K in Central Europe. The retrogression of initial positive Z500' over the eastern North Atlantic to Greenland along with a strengthening of negative Z500' over the southeastern North Atlantic around lag 15-25 days is striking. Furthermore, GL is associated with warm anomalies over Greenland and North America.

Finally, as expected by the varied regime succession for the SSWs with cyclonic regimes at their onset, composite temperature and Z500' are weaker for these events (Fig. 4c). Thus, the canonical response of surface temperature (i.e., the composite for all SSWs, Figure 4d) is the result of averaging over – in important regions opposing – temperature anomalies for SSWs with GL, EuBL, or a cyclonic regime at the onset.

6 Summary and Discussion

This study aimed to shed light on the large case-to-case variability of the tropospheric response to SSW events and their associated surface impacts, as well as the dependence on the tropospheric weather regime at the onset of the SSW. To that end, we have exploited in a statistical framework the observational record of the satellite era (1979 - 2019) as represented in the ERA-Interim reanalysis. Our conclusions are as follows:

1. In the aftermath of an SSW event, the tropospheric flow in the NAE region exhibits an evolution that is unlikely to occur in the absence of an SSW. Specifically, positive geopotential height anomalies related to Greenland blocking are statistically more likely to occur after the onset of the SSW than in the absence of an SSW. This is consistent with the expected (canonical) negative NAO response of the troposphere to SSWs (e.g. Charlton-Perez et al., 2018).

2. The significant and robust positive geopotential height anomalies found in the period 10-60 days after SSWs are predominantly the result of SSWs with European blocking at their onset. This is manifest for this subset of events in a transition from EuBL to GL that then dominates at lags of 15-20 and 30-55 days after the SSW onset, which is statistically significantly different from the natural progression from EuBL to GL. For other tropospheric regimes at SSW onset the tropospheric response is weaker and less robust and significant.

3. For Greenland blocking at the SSW onset, a weak preference for cyclonic flow regimes around 20-30 days after the SSW is apparent, with an opposite surface response in the aftermath of the SSW as compared to SSW onsets dominated by EuBL.

4. SSWs that occur during cyclonic weather regimes exhibit a considerably weaker and less significant response with a modestly enhanced likelihood for GL.

Depending on the tropospheric weather regime at SSW onset different surface signatures result. Specifically, the canonical signature in 2m temperature, e.g., cold conditions prevailing over much of northern Europe, occurs for the EuBL cases. In

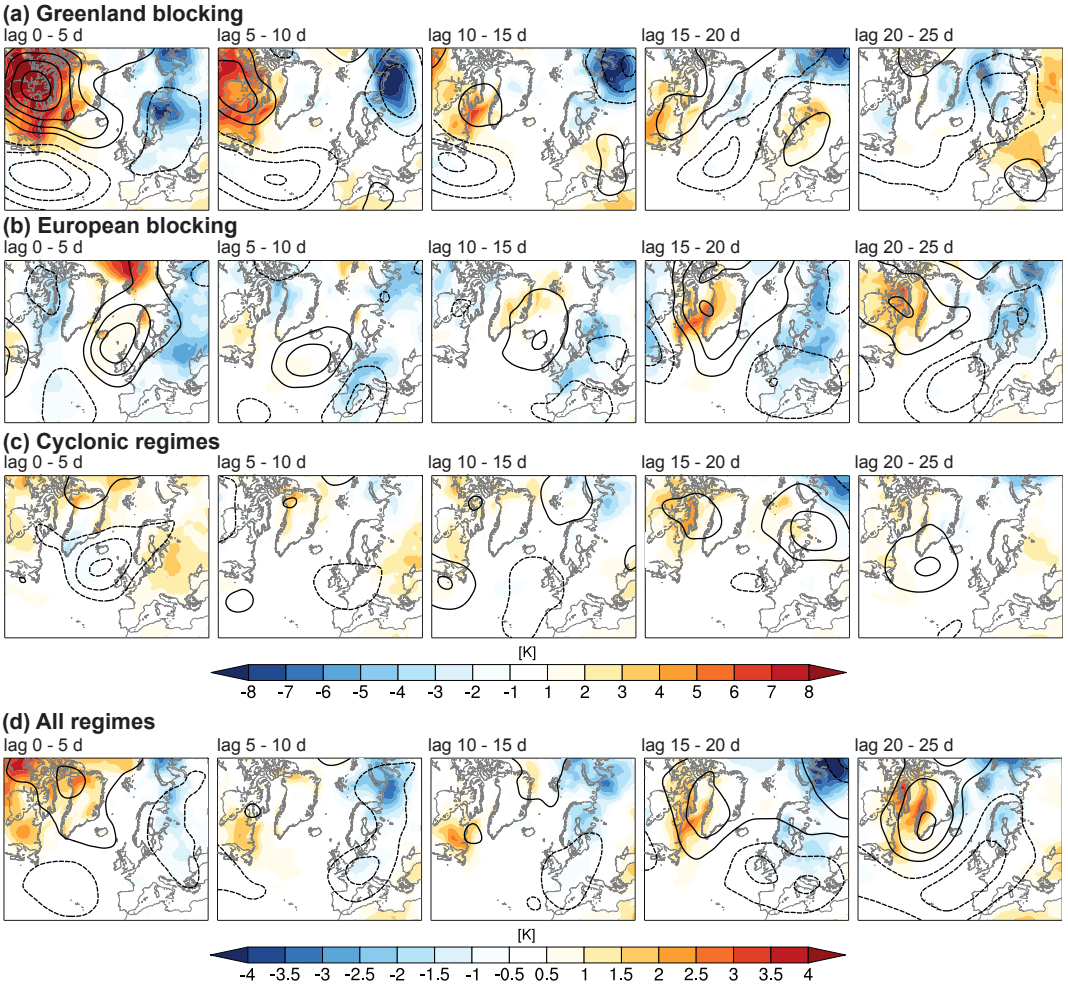

Figure 4. Surface impact for SSWs with (a) Greenland blocking, (b) European blocking, and (c) cyclonic regimes at the onset, as well as (d) for all SSWs. Shading indicates composite 2m temperature anomalies, black contours correspond to geopotential height anomalies at 500 hPa at intervals of (a-c) 50 gpm and (d) 25 gpm. Negative values are dashed. Fields are averaged over 5 days between lags 0 to 25 days. Note the different scales for temperature in (a-c) and (d).

contrast, mild temperatures in large parts of Europe are found for SSWs with GL at their onset. It is important to distinguish these cases, since although EuBL and GL frequently occur at the onset of SSW events, they lead to a different subsequent evolution and different associated surface temperatures. In particular, the most common transitions are from EuBL to GL and from GL to AT around 3-4 weeks after the SSW, respectively, along with their contrasting large-scale weather impacts (Beerli and Grams, 2019). These findings corroborate that the presence of either a EuBL or GL regime at SSW onset will allow us to disentangle the difference in surface weather, and hence to determine if and when a "downward impact" of the SSW is expected. This is highly relevant for subseasonal forecasting.

While these findings are limited by the small sample size of available SSW events, the rigorous statistical testing for significance and robustness performed here suggests that the large case-to-case variability in the tropospheric response to SSWs can be described in terms of NAE weather regimes and depends on the regime at the onset of the SSW. Our findings confirm that while the stratosphere does not represent the sole forcing of the tropospheric state, for many events it may be able to nudge the tropospheric flow into a particular direction by suppressing some weather regimes and by favoring others, as found in Charlton-Perez et al. (2018). We here in addition show that the susceptibility of the troposphere to the stratospheric nudging depends on the tropospheric state at the time of the SSW. Other factors that can modulate the tropospheric response are the persistence of the temperature anomaly in the lower stratosphere (Hitchcock et al., 2013a; Karpechko et al., 2017; Runde et al., 2016; Polichtchouk et al., 2018), as well as upstream effects in the eastern North Pacific (Afargan-Gerstman and Domeisen, 2020). An analysis of differences in the lower stratospheric persistence for the here considered weather regimes did not yield conclusive results, which warrants further studies. In particular, a model analysis to quantify the respective contributions to the tropospheric impact of different remote factors in comparison to the role of local North Atlantic variability might shed further light onto the complex role of stratosphere - troposphere coupling in surface weather.

However, it is currently not sufficiently known to what extent complex prediction models are able to represent the diversity of tropospheric responses to stratospheric forcing, as this has not been sufficiently tested in models beyond the canonical response and selected case studies. From a preliminary analysis of S2S prediction model data we anticipate large biases and a very complex role of the representation of stratosphere - troposphere coupling in prediction models that will be difficult to disentangle. Hence, while state-of-the-art subseasonal prediction systems are often unable to forecast at the time of occurrence of the SSW event if a surface response is to be expected, our findings suggests that the presence or absence – and in fact the timing – of a surface impact following SSW events might in some cases be predictable based on the weather regime at the onset of the SSW event. This could significantly improve the subseasonal prediction of tropospheric winter weather over Europe.

Data availability. The ERA-interim reanalysis data (Dee et al., 2011) is available from ECMWF at https://apps.ecmwf.int/datasets/data/interim-full-daily/.

Appendix A

Author contributions. The authors together initiated and designed the study and all authors contributed to data analysis, discussion of results, and writing.

Competing interests. The authors declare no competing interests.

Acknowledgements. Support from the Swiss National Science Foundation through project PP00P2_170523 to DD is gratefully acknowledged. The contribution of CMG was supported by the Helmholtz Association as part of the Young Investigator Group "SPREADOUT" (grant VH-NG-1243). Data analysis and visualisation were performed using the NCAR Command Language (UCAR/NCAR/CISL/VETS, 2014).

References

Afargan-Gerstman, H. and Domeisen, D. I. V.: Pacific Modulation of the North Atlantic Storm Track Response to Sudden Stratospheric Warming Events, Geophysical Research Letters, 47, 18, https://doi.org/https://doi.org/10.1029/2019GL085007, 2020.

Andrews, M. B., Knight, J. R., Scaife, A. A., and Lu, Y.: Observed and simulated teleconnections between the stratospheric Quasi-Biennial Oscillation and Northern Hemisphere winter atmospheric circulation, Journal of Geophysical Research – Atmospheres, https://doi.org/10.1029/2018JD029368, 2019.

Attard, H. E., Lang, A. L., Attard, H. E., and Lang, A. L.: The Impact of Tropospheric and Stratospheric Tropical Variability on the Location, Frequency, and Duration of Cool-Season Extratropical Synoptic Events, Monthly Weather Review, 147, 519–542, 2019.

Ayarzagüena, B., Barriopedro, D., Perez, J. M. G., Abalos, M., de la Camara, A., Herrera, R. G., Calvo, N., and Ordóñez, C.: Stratospheric Connection to the Abrupt End of the 2016/2017 Iberian Drought, Geophysical Research Letters, 45, 12,639–12,646, 2018.

Baldwin, M. P. and Dunkerton, T. J.: Stratospheric harbingers of anomalous weather regimes, Science, 294, 581–584, 2001.

Barnes, E. A., Samarasinghe, S. M., Uphoff, I. E., and Furtado, J. C.: Tropospheric and Stratospheric Causal Pathways Between the MJO and NAO, Journal of Geophysical Research-Atmospheres, 124, 9356–9371, 2019.

Beerli, R. and Grams, C. M.: Stratospheric Modulation of the Large-Scale Circulation in the Atlantic-European Region and Its Implications for Surface Weather Events, Quarterly Journal of the Royal Meteorological Society, 0, https://doi.org/10.1002/qj.3653, 2019.

Beerli, R., Wernli, H., and Grams, C. M.: Does the lower stratosphere provide predictability for month-ahead wind electricity generation in Europe?, Quarterly Journal of the Royal Meteorological Society, 143, 3025–3036, 2017.

Butler, A., Charlton-Perez, A., Domeisen, D. I. V., Garfinkel, C., Gerber, E. P., Hitchcock, P., Karpechko, A. Y., Maycock, A. C., Sigmond, M., Simpson, I., and Son, S.-W.: Sub-seasonal Predictability and the Stratosphere, in: Sub-Seasonal to Seasonal Prediction, pp. 223–241, Elsevier, https://doi.org/10.1016/B978-0-12-811714-9.00011-5, 2019.

Butler, A. H., Arribas, A., Athanassiadou, M., Baehr, J., Calvo, N., Charlton-Perez, A., Déqué, M., Domeisen, D. I. V., Fröhlich, K., Hendon, H., Imada, Y., Ishii, M., Iza, M., Karpechko, A. Y., Kumar, A., MacLachlan, C., Merryfield, W. J., Müller, W. A., O'Neill, A., Scaife, A. A., Scinocca, J., Sigmond, M., Stockdale, T. N., and Yasuda, T.: The Climate-system Historical Forecast Project: do stratosphere-resolving models make better seasonal climate predictions in boreal winter?, Quarterly Journal of the Royal Meteorological Society, 142, 1413–1427, 2016.

Butler, A. H., Sjoberg, J. P., Seidel, D. J., and Rosenlof, K. H.: A sudden stratospheric warming compendium, Earth System Science Data, 9, 63–76, 2017.

Charlton, A. and Polvani, L.: A new look at stratospheric sudden warmings. Part I: Climatology and modeling benchmarks, J. Climate, 20, 449–469, 2007.

Charlton-Perez, A. J., Ferranti, L., and Lee, R. W.: The influence of the stratospheric state on North Atlantic weather regimes, Quarterly Journal of the Royal Meteorological Society, 144, 1140–1151, 2018.

Cohen, J., Furtado, J. C., Jones, J., Barlow, M., Whittleston, D., and Entekhabi, D.: Linking Siberian Snow Cover to Precursors of Stratospheric Variability, Journal of Climate, 27, 5422–5432, 2014.

Dee, D., Uppala, S., Simmons, A., Berrisford, P., Poli, P., Kobayashi, S., Andrae, U., Balmaseda, M., Balsamo, G., Bauer, P., Bechtold, P., Beljaars, A., Berg, L., Bidlot, J., Bormann, N., Delsol, C., Dragani, R., Fuentes, M., Geer, A., Haimberger, L., Healy, S., Hersbach, H., Holm, E., Isaksen, L., Kållberg, P., Köhler, M., Matricardi, M., McNally, A., Monge-Sanz, B., Morcrette, J., Park, B., Peubey, C., Rosnay,

P. d., Tavolato, C., Thepaut, J., and Vitart, F.: The ERA-Interim reanalysis: Configuration and performance of the data assimilation system, Q. J. Royal Met. Soc., 137, 553–597, 2011.

Domeisen, D. I. V.: Estimating the Frequency of Sudden Stratospheric Warming Events from Surface Observations of the North Atlantic Oscillation, Journal of Geophysical Research-Atmospheres, 124, https://doi.org/10.1029/2018JD030077, 2019.

Domeisen, D. I. V., Sun, L., and Chen, G.: The role of synoptic eddies in the tropospheric response to stratospheric variability, Geophys. Res. Lett., 40, 4933–4937, https://doi.org/10.1002/grl.50943, 2013.

Domeisen, D. I. V., Butler, A. H., Fröhlich, K., Bittner, M., Müller, W. A., and Baehr, J.: Seasonal Predictability over Europe Arising from El Niño and Stratospheric Variability in the MPI-ESM Seasonal Prediction System, Journal of Climate, 28, 256–271, https://doi.org/10.1175/JCLI-D-14-00207.1, 2015.

Domeisen, D. I. V., Garfinkel, C. I., and Butler, A. H.: The Teleconnection of El Niño Southern Oscillation to the Stratosphere, Reviews of Geophysics, 57, https://doi.org/10.1029/2018RG000596, 2019.

Domeisen, D. I. V., Butler, A. H., Charlton-Perez, A. J., Ayarzaguena, B., Baldwin, M. P., Dunn Sigouin, E., Furtado, J. C., Garfinkel, C. I., Hitchcock, P., Karpechko, A. Y., Kim, H., Knight, J., Lang, A. L., Lim, E.-P., Marshall, A., Roff, G., Schwartz, C., Simpson, I. R., Son, S.-W., and Taguchi, M.: The role of the stratosphere in subseasonal to seasonal prediction. Part 2: Predictability arising from stratosphere - troposphere coupling, Journal of Geophysical Research-Atmospheres, https://doi.org/10.1029/2019JD030923, 2020a.

Domeisen, D. I. V., Butler, A. H., Charlton-Perez, A. J., Ayarzaguena, B., Baldwin, M. P., Dunn Sigouin, E., Furtado, J. C., Garfinkel, C. I., Hitchcock, P., Karpechko, A. Y., Kim, H., Knight, J., Lang, A. L., Lim, E.-P., Marshall, A., Roff, G., Schwartz, C., Simpson, I. R., Son, S.-W., and Taguchi, M.: The role of the stratosphere in subseasonal to seasonal prediction. 1. Predictability of the stratosphere, Journal of Geophysical Research-Atmospheres, https://doi.org/10.1029/2019JD030920, 2020b.

Drouard, M., Rivière, G., Arbogast, P., Drouard, M., Rivière, G., and Arbogast, P.: The North Atlantic Oscillation Response to Large-Scale Atmospheric Anomalies in the Northeastern Pacific, dx.doi.org, 70, 2854–2874, 2013.

Ferranti, L., Corti, S., and Janousek, M.: Flow-Dependent Verification of the ECMWF Ensemble over the Euro-Atlantic Sector, Quarterly Journal of the Royal Meteorological Society, 141, 916–924, https://doi.org/10.1002/qj.2411, 2015.

Garfinkel, C. I., Waugh, D. W., and Gerber, E. P.: The Effect of Tropospheric Jet Latitude on Coupling between the Stratospheric Polar Vortex and the Troposphere, Journal of Climate, 26, 2077–2095, 2013.

Garfinkel, C. I., Benedict, J. J., and Maloney, E. D.: Impact of the MJO on the boreal winter extratropical circulation, Geophysical Research Letters, 41, 6055–6062, 2014.

Gerber, E. P., Orbe, C., and Polvani, L. M.: Stratospheric influence on the tropospheric circulation revealed by idealized ensemble forecasts, Geophysical Research Letters, 36, L24 801, 2009.

Grams, C. M., Beerli, R., Pfenninger, S., Staffell, I., and Wernli, H.: Balancing Europe's wind-power output through spatial deployment informed by weather regimes, Nature Climate Change, 7, nclimate3338–562, 2017.

Gray, L. J., Anstey, J. A., Kawatani, Y., Lu, H., Osprey, S., and Schenzinger, V.: Surface impacts of the Quasi Biennial Oscillation, Atmospheric Chemistry And Physics, 18, 8227–8247, 2018.

Greatbatch, R. J., Gollan, G., Jung, T., and Kunz, T.: Factors influencing Northern Hemisphere winter mean atmospheric circulation anomalies during the period 1960/61 to 2001/02, Quarterly Journal of the Royal Meteorological Society, 138, 1970–1982, 2012.

Hitchcock, P. and Simpson, I. R.: The Downward Influence of Stratospheric Sudden Warmings, J. Atmos. Sci., 71, 3856–3876, 2014.

Hitchcock, P., Shepherd, T. G., and Manney, G. L.: Statistical Characterization of Arctic Polar-Night Jet Oscillation Events, Journal of Climate, 26, 2096–2116, 2013a.

Hitchcock, P., Shepherd, T. G., Taguchi, M., Yoden, S., and Noguchi, S.: Lower-stratospheric Radiative Damping and Polar-night Jet Oscillation Events, J. Atmos. Sci., 70, 1391–1408, 2013b.

Honda, M. and Nakamura, H.: Interannual Seesaw between the Aleutian and Icelandic Lows. Part II: Its Significance in the Interannual Variability over the Wintertime Northern Hemisphere, Journal of Climate, 14, 4512–4529, 2001.

Huang, J. and Tian, W.: Eurasian Cold Air Outbreaks under Different Arctic Stratospheric Polar Vortex Strength, Journal of the Atmospheric Sciences, https://doi.org/10.1175/JAS-D-18-0285.1, 2019.

Jia, L., Yang, X., Vecchi, G., Gudgel, R., Delworth, T., Fueglistaler, S., Lin, P., Scaife, A. A., Underwood, S., and Lin, S.-J.: Seasonal Prediction Skill of Northern Extratropical Surface Temperature Driven by the Stratosphere, Journal of Climate, 30, 4463–4475, 2017.

Jiménez-Esteve, B. and Domeisen, D. I. V.: The Tropospheric Pathway of the ENSO-North Atlantic Teleconnection, Journal of Climate, 31, 4563–4584, https://doi.org/10.1175/JCLI-D-17-0716.1, 2018.

Karpechko, A. Y.: Improvements in statistical forecasts of monthly and two-monthly surface air temperatures using a stratospheric predictor, Quarterly Journal of the Royal Meteorological Society, 141, 2444–2456, 2015.

Karpechko, A. Y., Hitchcock, P., Peters, D. H. W., and Schneidereit, A.: Predictability of downward propagation of major sudden stratospheric warmings, Q. J. Royal Met. Soc., 104, 30 937, 2017.

Kodera, K., Mukougawa, H., Maury, P., Ueda, M., and Claud, C.: Absorbing and reflecting sudden stratospheric warming events and their relationship with tropospheric circulation, Journal of Geophysical Research-Atmospheres, 121, 80–94, 2016.

Kolstad, E. W., Breiteig, T., and Scaife, A. A.: The association between stratospheric weak polar vortex events and cold air outbreaks in the Northern Hemisphere, Quarterly Journal of the Royal Meteorological Society, 136, 886–893, 2010.

Kretschmer, M., Cohen, J., Matthias, V., Runge, J., and Coumou, D.: The Different Stratospheric Influence on Cold-Extremes in Eurasia and North America, npj Climate and Atmospheric Science, 1, 44, https://doi.org/10.1038/s41612-018-0054-4, 2018a.

Kretschmer, M., Coumou, D., Agel, L., Barlow, M., Tziperman, E., and Cohen, J.: More-Persistent Weak Stratospheric Polar Vortex States Linked to Cold Extremes, Bulletin of the American Meteorological Society, 99, 49–60, 2018b.

Kuroda, Y. and Kodera, K.: Role of the Polar-night Jet Oscillation on the formation of the Arctic Oscillation in the Northern Hemisphere winter, Journal of Geophysical Research, 109, D11 112, 2004.

Martius, O., Polvani, L., and Davies, H.: Blocking precursors to stratospheric sudden warming events, Geophys. Res. Lett., 36, L14 806, 2009.

Maycock, A. C. and Hitchcock, P.: Do split and displacement sudden stratospheric warmings have different annular mode signatures?, Geophysical Research Letters, 42, 10 943–10 951, 2015.

Maycock, A. C., Masukwedza, G. I. T., Hitchcock, P., and Simpson, I. R.: A Regime Perspective on the North Atlantic Eddy-Driven Jet Response to Sudden Stratospheric Warmings, Journal of Climate, 33, 3901–3917, 2020.

Michel, C. and Rivière, G.: The Link between Rossby Wave Breakings and Weather Regime Transitions, Journal of the Atmospheric Sciences, 68, 1730–1748, https://doi.org/10.1175/2011JAS3635.1, 2011.

Michelangeli, P.-A., Vautard, R., and Legras, B.: Weather Regimes: Recurrence and Quasi Stationarity, Journal of the Atmospheric Sciences, 52, 1237–1256, https://doi.org/10.1175/1520-0469(1995)052<1237:WRRAQS>2.0.CO;2, 1995.

Mitchell, D. M., Gray, L. J., Anstey, J., Baldwin, M. P., and Charlton-Perez, A. J.: The Influence of Stratospheric Vortex Displacements and Splits on Surface Climate, Journal of Climate, 26, 2668–2682, 2013.

Nakagawa, K. I. and Yamazaki, K.: What kind of stratospheric sudden warming propagates to the troposphere?, Geophysical Research Letters, 33, 30 937–4, 2006.

Nishii, K., Nakamura, H., and Orsolini, Y. J.: Geographical Dependence Observed in Blocking High Influence on the Stratospheric Variability through Enhancement and Suppression of Upward Planetary-Wave Propagation, J. Climate, 24, 6408–6423, 2011.

Papritz, L. and Grams, C.: Linking low-frequency large-scale circulation patterns to cold air outbreak formation in the north-eastern North Atlantic, Geophys. Res. Lett., 45, 2542–2553, https://doi.org/10.1002/2017GL076921, 2018.

Peings, Y.: Ural Blocking as a driver of early winter stratospheric warmings, Geophysical Research Letters, pp. 2019GL082 097–18, 2019.

Polichtchouk, I., Shepherd, T. G., and Byrne, N. J.: Impact of Parametrized Nonorographic Gravity Wave Drag on Stratosphere-Troposphere Coupling in the Northern and Southern Hemispheres, Geophysical Research Letters, 45, 8612–8618, 2018.

Runde, T., Dameris, M., Garny, H., and Kinnison, D. E.: Classification of stratospheric extreme events according to their downward propagation to the troposphere, Geophysical Research Letters, 43, 6665–6672, 2016.

Scaife, A. A., Karpechko, A. Y., Baldwin, M. P., Brookshaw, A., Butler, A. H., Eade, R., Gordon, M., MacLachlan, C., Martin, N., Dunstone, N., and Smith, D.: Seasonal winter forecasts and the stratosphere, Atmospheric Science Letters, 17, 51–56, 2016.

Seviour, W. J. M., Gray, L. J., and Mitchell, D. M.: Stratospheric polar vortex splits and displacements in the high-top CMIP5 climate models, Journal of Geophysical Research-Atmospheres, pp. 1–14, 2016.

Sigmond, M., Scinocca, J. F., Kharin, V. V., and Shepherd, T. G.: Enhanced seasonal forecast skill following stratospheric sudden warmings, Nature Geoscience, 6, 1–5, 2013.

Smith, K. L. and Scott, R. K.: The role of planetary waves in the tropospheric jet response to stratospheric cooling, Geophysical Research Letters, 43, 2904–2911, 2016.

Song, Y. and Robinson, W. A.: Dynamical Mechanisms for Stratospheric Influences on the Troposphere, Journal of the Atmospheric Sciences, 61, 1711–1725, 2004.

Sun, J. and Tan, B.: Mechanism of the wintertime Aleutian Low–Icelandic Low seesaw, Geophysical Research Letters, 40, 4103–4108, 2013.

Sun, L., Deser, C., and Tomas, R. A.: Mechanisms of Stratospheric and Tropospheric Circulation Response to Projected Arctic Sea Ice Loss*, Journal of Climate, 28, 7824–7845, 2015.

Taguchi, M.: Predictability of Major Stratospheric Sudden Warmings of the Vortex Split Type: Case Study of the 2002 Southern Event and the 2009 and 1989 Northern Events, J. Atmos. Sci., 71, 2886–2904, 2014.

Taguchi, M.: Connection of predictability of major stratospheric sudden warmings to polar vortex geometry, Atmospheric Science Letters, 17, 33–38, 2016.

Tyrrell, N. L., Karpechko, A. Y., Uotila, P., and Vihma, T.: Atmospheric Circulation Response to Anomalous Siberian Forcing in October 2016 and its Long-Range Predictability, Geophysical Research Letters, 104, 30,937–11, 2019.

UCAR/NCAR/CISL/VETS: The NCAR Command Language (Version 6.1.2) [Software], Boulder, Colorado, https://doi.org/http://dx.doi.org/10.5065/D6WD3XH5, http://www.ncl.ucar.edu/, 2014.

Vautard, R.: Multiple Weather Regimes over the North Atlantic: Analysis of Precursors and Successors, Monthly Weather Review, 118, 2056–2081, https://doi.org/10.1175/1520-0493(1990)118<2056:MWROTN>2.0.CO;2, 1990.

White, I., Garfinkel, C. I., Gerber, E. P., Jucker, M., Aquila, V., and Oman, L. D.: The Downward Influence of Sudden Stratospheric Warmings: Association with Tropospheric Precursors, Journal of Climate, 32, 85–108, 2019.

Woollings, T., Charlton-Perez, A., Ineson, S., Marshall, A. G., and Masato, G.: Associations between stratospheric variability and tropospheric blocking, J. Geophys. Res.: Atmospheres, 115, D06 108, 2010.

Zhang, R., Tian, W., Zhang, J., Huang, J., Xie, F., and Xu, M.: The Corresponding Tropospheric Environments during Downward-extending and Non-downward-extending Events of Stratospheric Northern Annular Mode Anomalies, Journal of Climate, pp. JCLI–D–18–0574.1, 2019.

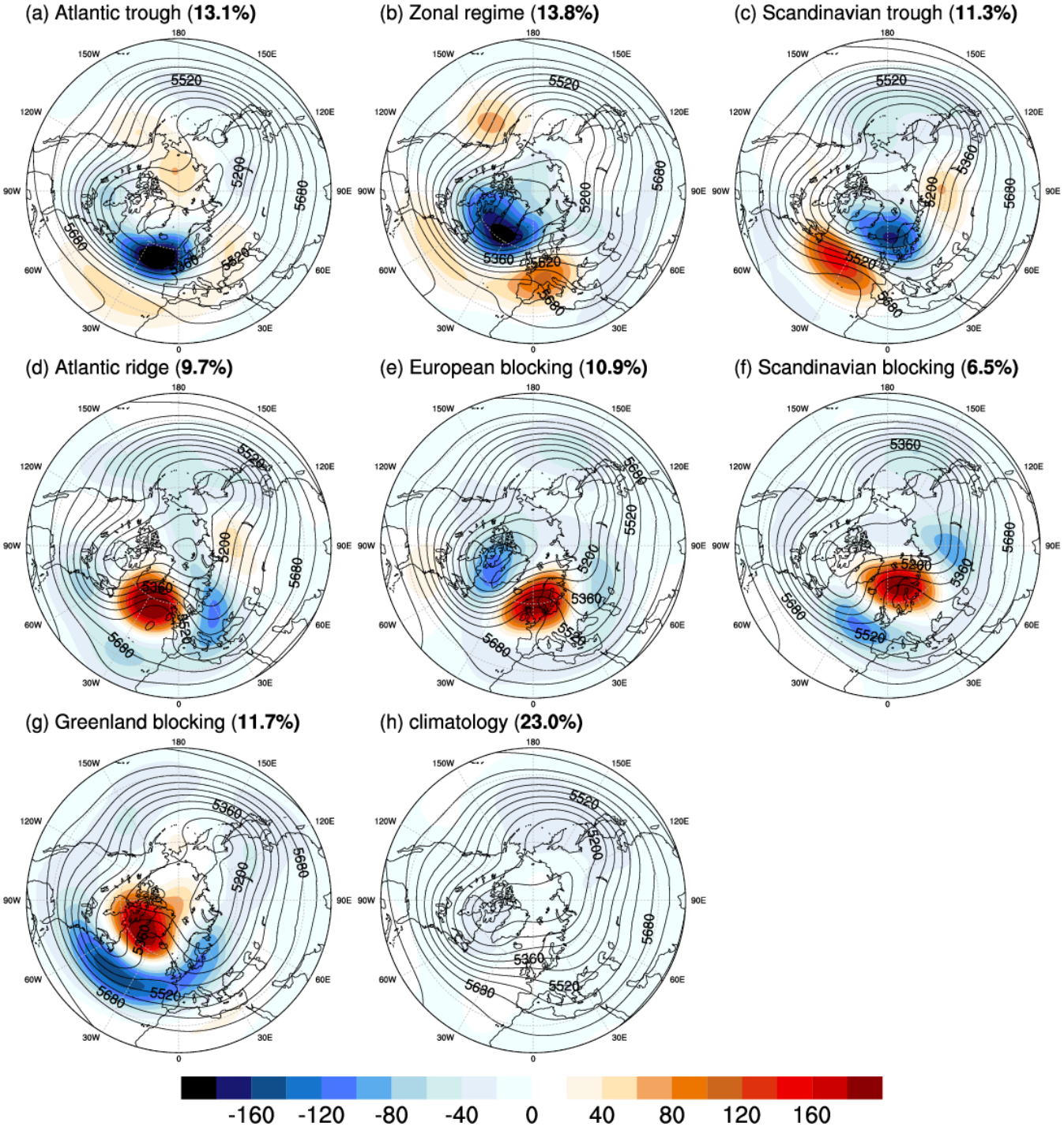

Figure A1. Composite mean 10-day low-pass filtered 500 hPa geopotential height anomaly (shading, every 20 gpm), and mean absolute 500 hPa geopotential height (black contours, every 20 gpm) for all winter days in ERA-Interim (DJF, 1979-2015) attributed to one of the 7 weather regimes (a-g) and the climatological mean (h). Regime name and relative frequency (in percent) are indicated in the sub-figure captions.

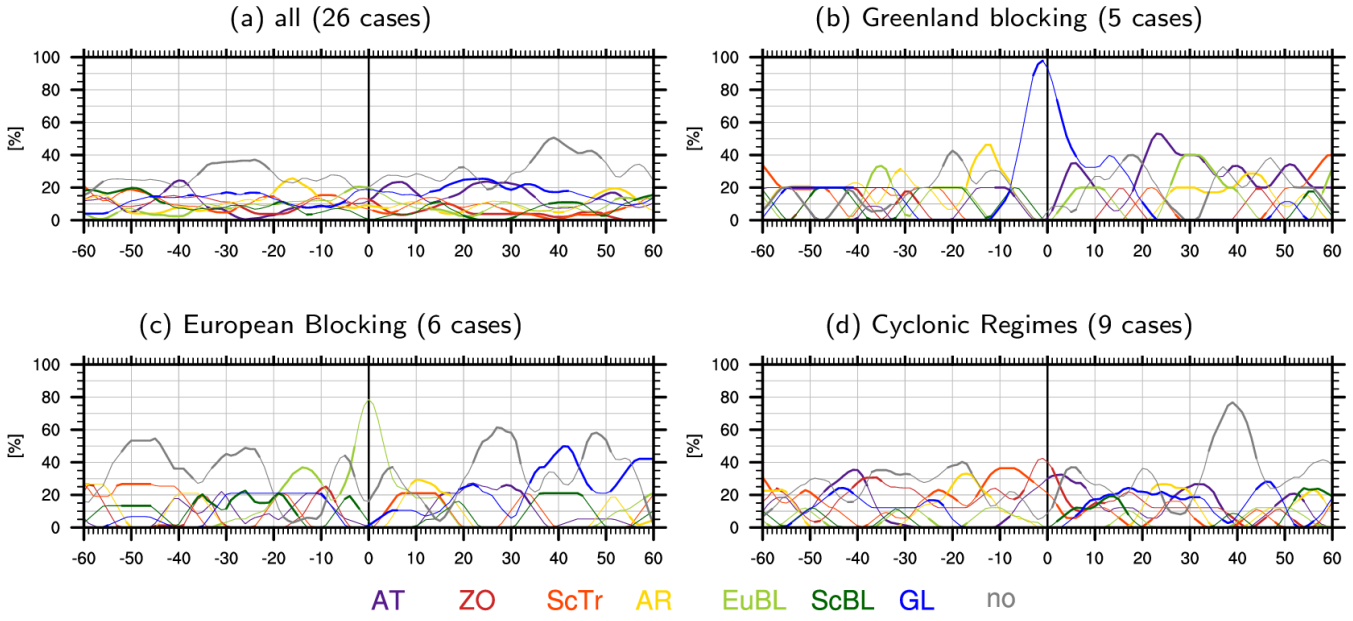

Figure A2. As Figure 2 but for the 5-day running mean *absolute* frequency of weather regimes centred on the onset of the SSW event (lag 0) for (a) all SSW events and (b-d) conditional on the dominant weather regime at lag 0: (b) Greenland blocking, (c) European blocking, and (d) cyclonic regimes (ZO, AT, and ScTr). The 5-day mean frequencies are computed from 6-hourly weather regime data from lag -60 days to lag 60 days. Note the different y-axis in (a). The bold parts of the lines indicate significant deviations from climatology (see text for details).

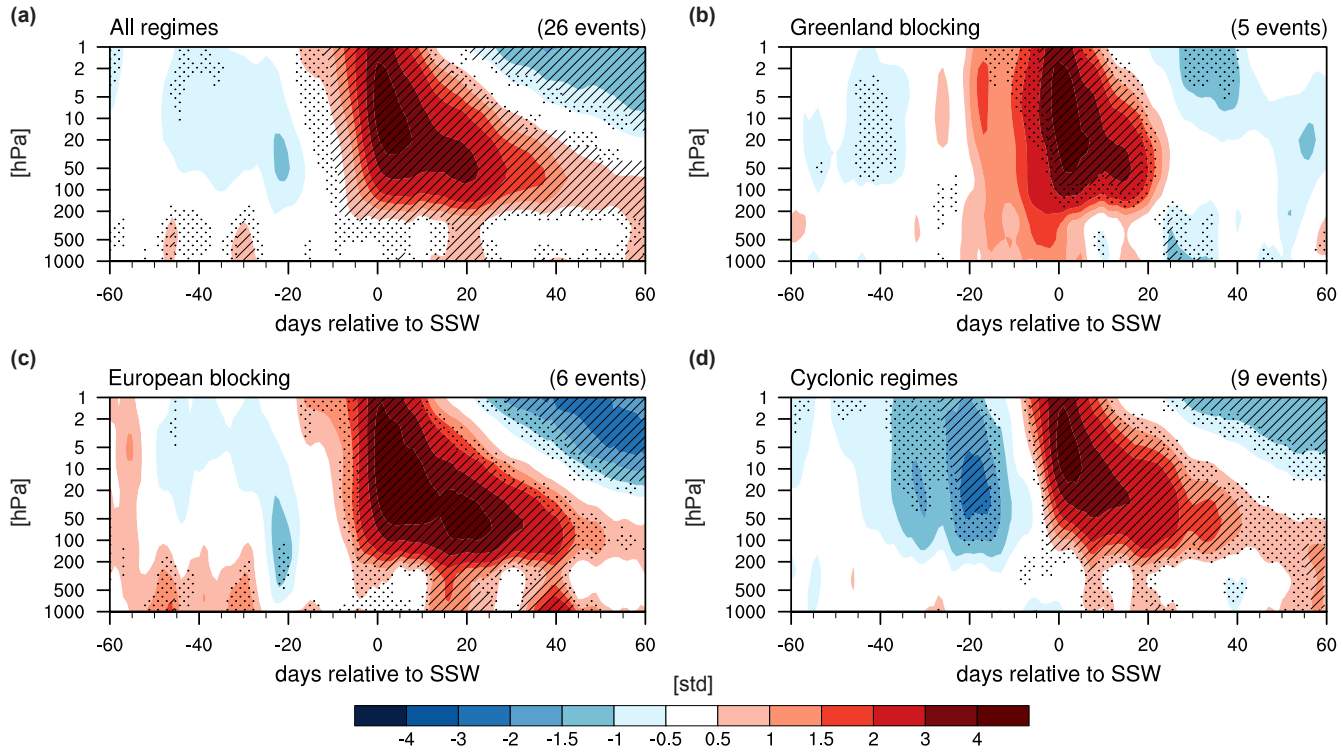

Figure A3. As Figure 3 but for the full longitude range, i.e. for the polar cap poleward of 60°N.

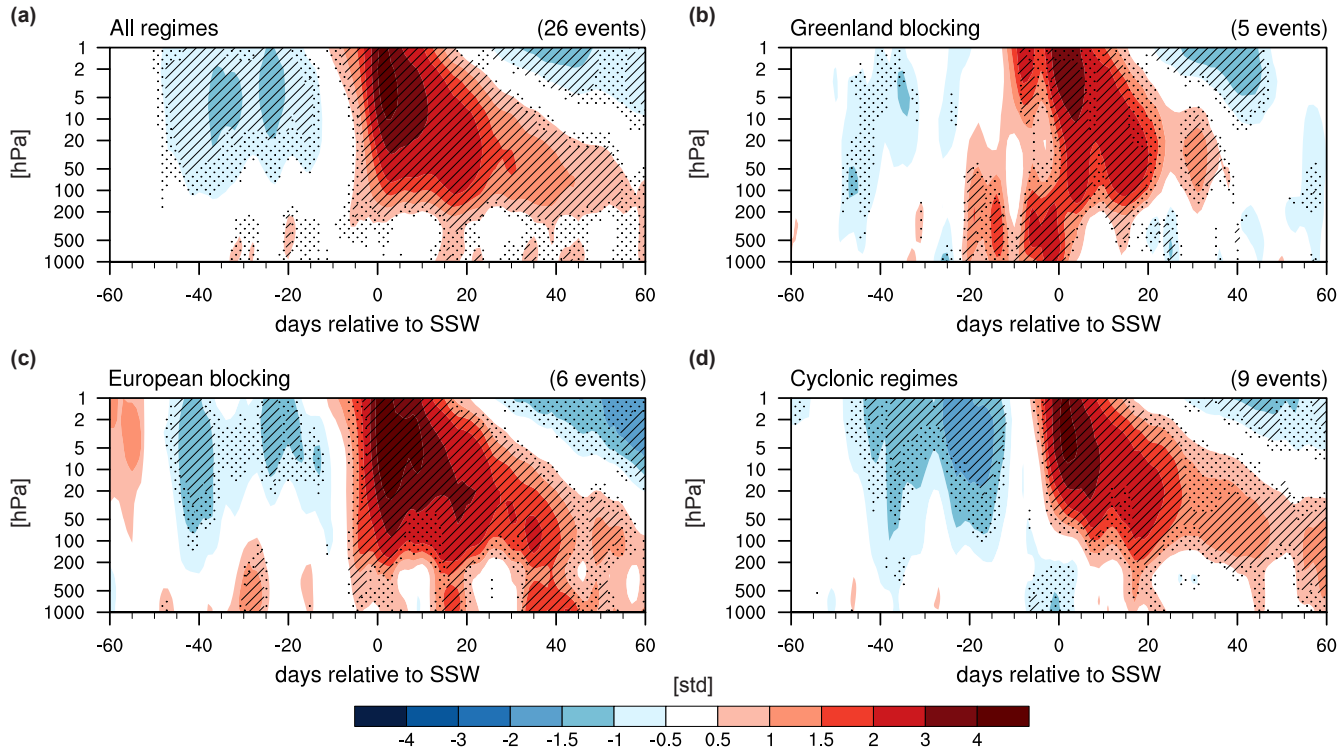

Figure A4. Standardized geopotential height anomalies for the sector -80°E to 40°E / 60°N to 90°N for (a) all SSW events, and (b-d) sub-divided by the weather regime that is dominant at the onset of the SSW as indicated by the titles of the panels. Robustness is assessed using confidence intervals by resampling the SSW events 100 times with repetition. If the magnitude of the anomaly exceeds the interquartile or the 10^{th}-90^{th} percentile ranges the anomaly is highlighted by stippling or hatching, respectively. See Section 2.2 for details.

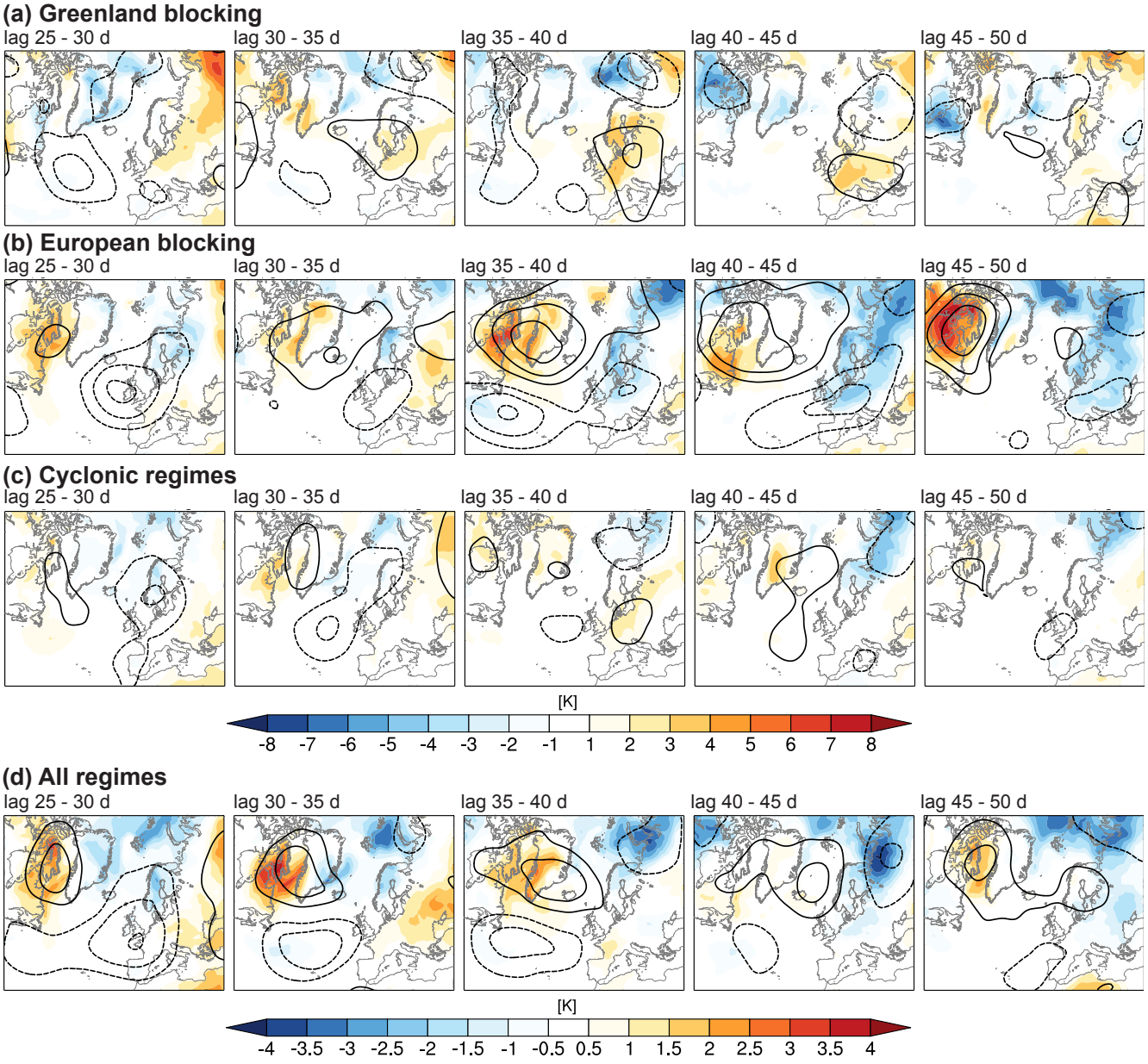

Figure A5. As Fig. 4 but for days 25 - 50.